

# Complete analysis of the BEAVRS benchmark using the GPU-based direct whole core calculation code CRANE\*

Jun Li,<sup>1</sup> Guo-Hua Chen,<sup>2,3</sup> Qian Zhang,<sup>1</sup> Ruo-Han Zheng,<sup>4</sup> Li-Qin Zhang,<sup>4</sup> and Shao-Hong Zhang<sup>1,†</sup>

<sup>1</sup>*School of Physics, Zhejiang University, Hangzhou, 310027, China*

<sup>2</sup>*Shanghai NuStar Nuclear Power Technology Co. Ltd, Shanghai, 201101, China*

<sup>3</sup>*Advanced Technology Institute, Zhejiang University, Hangzhou, 310027, China*

<sup>4</sup>*Nuclear Power Institute of China, Chengdu, 610041, China*

The BEAVRS (Benchmark for Evaluation and Validation of Reactor Simulation) benchmark problem proposed by the Massachusetts Institute of Technology (MIT) computational reactor physics group is widely used by various institutions in the world to verify and validate their new generation direct whole core calculation codes. It enables analysts to develop an extremely detailed PWR core model, and carry out multi-physics coupled verification and validation for the reactor core analysis code. Although there are numerous publications in the literature reporting the validation results, few publishes a thorough validation results against all the measurement data of the problem. In this paper, the BEAVRS problem is solved using the CRANE code, which is a fully GPU-based deterministic direct whole core calculation code for PWR. It is demonstrated that direct whole core calculation with detailed core model can be performed on a mini server mounted with 10 consumer-grade RTX 3090 graphics cards, and the average time needed to complete neutronics and thermal hydraulics coupled analysis for single core state is just about one minute. Thorough verification and validation against all the measurement data shows that the predicted criticality, control rod bank worths, in-core detector signal distribution and the boron let-down curves of two cycles agree well with the measurements. These results indicate that even by exploiting the computing power of consumer-grade GPUs, direct whole core calculations with detailed core model for large commercial PWRs are now practically possible, and CRANE is ready for PWR practical applications in terms of both solution fidelity and speed performance.

Keywords: BEAVRS benchmark, direct whole core calculation, CRANE, GPU computation

## I. INTRODUCTION

1 A nuclear reactor is a typical complex system with multi-  
2 physics coupling. Due to the high cost of conducting nuclear  
3 reactor experimental research, numerical simulation has al-  
4 ways been an important means of investigating the behav-  
5 ior of nuclear reactors. With the rapid development of com-  
6 puter hardware performance, since the beginning of this cen-  
7 tury, researchers have made significant progress in conduct-  
8 ing first-principle-based simulations of the multi-physics be-  
9 haviors in nuclear reactors. A batch of new generation codes  
10 have been successfully developed, adopting either the deter-  
11 ministic approach or the probabilistic approach. For instance,  
12 code DeCART[1], nTRACER[2], MPACT[3], and NECP-  
13 X[4] are the deterministic ones primarily based on the method  
14 of characteristic (MOC) while code MC21[5], RMC [6] and  
15 OpenMC[7], JMCT[8] are the probabilistic ones employing  
16 the Monte Carlo (MC) method. All these codes are able  
17 to perform high-fidelity direct whole core calculations for  
18 PWRs without introducing any empirical hypothesis as in the  
19 conventional two-step analysis method.

20 BEAVRS [9] is a benchmark problem proposed by the MIT  
21 Computational Reactor Physics Group in 2013 to meet the  
22 needs of verifying and validating the new generation of reac-  
23 tor core analysis codes. This problem is based on a 4-loop

25 pressurized water reactor designed by Westinghouse in the  
26 United States. It provides highly detailed as-is design data for  
27 the reactor and also measurement data for the initial two op-  
28 erating cycles to the public to allow for validation of methods  
29 developments. It enables analysts to develop an extremely de-  
30 tailed PWR core model, and carry out multi-physics coupled  
31 verification and validation for the reactor core analysis code.  
32 Since the previous light water reactor benchmarks can only be  
33 used to verify a single physical problem, and most of the in-  
34 stitutions cannot have access to this kind of utility proprietary  
35 information, this problem is unique and valuable.

36 Considering the complexity of the problem and the com-  
37 putation cost that it would take to perform direct whole core  
38 multi-physics coupled calculation with very detailed core  
39 modeling, it is a challenging task to complete the high-fidelity  
40 analysis of the problem. So far, various institutions in the  
41 world have attempted to solve this problem using their new  
42 generation codes. However, the degree of completion for  
43 this problem varies among the institutions. Some have only  
44 completed the calculation for the zero power state at the be-  
45 ginning of the first cycle (BOC1), while others have com-  
46 pleted both the BOC1 calculation and the first cycle core fol-  
47 low calculations. Only a few institutions have completed all  
48 the two cycles calculation provided in the benchmark prob-  
49 lem. While for the validation of computational results against  
50 the measurement data, the degree of completion also varies  
51 among institutions. Most institutions have conducted com-  
52 parisons of BOC1 critical boron concentrations and the boron  
53 letdown curve for the initial cycle, while only a few have car-  
54 ried out comparisons of control rod bank worth and in-core  
55 flux measurement results at different burnup of the reactor.  
56 So far, there is no literature published yet reporting the com-

\* The work was granted by Nuclear Power Technology Innovation Center of China [Grant number: HDLCXZX-2022-HD-011].

† Corresponding author, Shao-Hong Zhang, School of Physics, Zhejiang University, Hangzhou, 310027, China. E-mail: zhangshh@zju.edu.cn

57 parison of control rod bank worth between the prediction and  
 58 the measurement data obtained at the low-power physics test  
 59 (LPPT) stage at the beginning of Cycle 2. Moreover, since the  
 60 target computing platform for most of today's direct whole  
 61 core calculation codes are CPU-based dedicated supercom-  
 62 puters, it is impractical for them to exactly follow the reactor  
 63 power history due to the large computational cost required,  
 64 people have to adopt the simplified or approximated power  
 65 history when using these codes to perform the core follow  
 66 calculation.

67 This work focuses on using the fully GPU-based deter-  
 68 ministic direct whole core calculation code CRANE[10] to  
 69 analyze the BEAVRS benchmark problem for assessing its  
 70 solution fidelity and speed performance for PWR practical  
 71 applications. It will be demonstrated that just by exploiting  
 72 the computing power of consumer-grade GPUs, direct whole  
 73 core calculation with detailed core model and reactor core fol-  
 74 low calculation adopting the exact reactor power operation  
 75 history are now practical possible. Thorough verification and  
 76 validation of CRANE prediction results against all the mea-  
 77 surement data of the benchmark problem will also be per-  
 78 formed, parameters such as the control rod bank worth at the  
 79 beginning of the second cycle, which have not been reported  
 80 in previous literature, will also be presented with comparative  
 81 results in this work.

82 The rest of the paper is organized as follows. Section II  
 83 outlines the methodology that CRANE adopted for PWR neu-  
 84 tronics, thermal hydraulics and fuel rod performance coupled  
 85 calculation. Section III gives the necessary details about the  
 86 CRANE BEAVRS core modeling. Section IV presents the  
 87 validation results against all the measurement data from the  
 88 two operating cycles of the problem, and also the compar-  
 89 isons of prediction accuracy of CRANE with that of rele-  
 90 vant codes in the world. Section V gives the introduction of  
 91 the CPU-GPU heterogenous hardware adopted for this study  
 92 and the superior speed performance obtained by exploiting  
 93 the computing power of today's consumer-grade GPUs, while  
 94 Section VI concludes the paper.

## 95 II. CRANE METHODOLOGY

96 CRANE is an advanced deterministic direct whole core  
 97 calculation code for PWRs. It has been developed in Shang-  
 98 hai NuStar Nuclear Power Technology Co., Ltd for several  
 99 years as its next generation core analysis code targeting for  
 100 commercial PWR applications. The code is able to perform  
 101 high-fidelity reactor neutronics and thermal hydraulics cou-  
 102 pled analysis. The main methodology implemented in the  
 103 code is outlined in this section.

104 The neutronics module of CRANE has extensively inher-  
 105 ited many methods and good practice from NuStar's 2D lat-  
 106 tice physics code ROBIN[11], such as the 69-group cross sec-  
 107 tion data library processed from the ENDF/B-VII.1 evaluated  
 108 nuclear data file, the resonance calculation method applica-  
 109 ble to the irregular geometries that integrates the traditional  
 110 equivalence theory and the enhanced neutron current method,  
 111 the use of pre-calculated correction factor tables to account

112 for the resonance interference effects among major resonant  
 113 nuclei. To achieve a three-dimensional neutron transport so-  
 114 lution for the entire reactor with a fine resolution down to the  
 115 sub-pin level, the 2D/1D coupled iteration method is adopted.  
 116 MOC (Method of Characteristics) method is employed to  
 117 solve both the 2D planar problem and also the axial 1D prob-  
 118 lem. Iteration acceleration is achieved by successively solv-  
 119 ing the pin-level multi-group and few-group partial current-  
 120 based 3D Coarse Mesh Finite Difference (pCMFD) problem.  
 121 Implicit trapezoidal method and Chebyshev rational approxi-  
 122 mation (CRAM) are used to solve the depletion problem, and  
 123 the strategy of linear reaction rate method (LR) and logarith-  
 124 mic linear reaction rate method (LLR) are used to deal with  
 125 the coupling calculation of neutron transport and depletion  
 126 for normal fuel pins and Gd-bearing fuel pins respectively.

127 The thermal-hydraulic module of CRANE includes a sub-  
 128 channel analysis model for calculating the temperature and  
 129 density of the coolant, as well as a fuel rod analysis model  
 130 for calculating the temperature of the fuel pellet. The sub-  
 131 channel analysis model is developed with reference to the  
 132 CTF code[12], it gives the temperature and density of the  
 133 coolant around the fuel rod by solving the mass, energy, and  
 134 momentum conservation equations for the two-fluid, three-  
 135 field (i.e. fluid film, fluid drops, and vapor) system within  
 136 the pin-level sub-channel control volumes. While the fuel rod  
 137 analysis model is developed by employing the fuel perfor-  
 138 mance analysis model that the FuSPAC code[13] used. Fuel  
 139 rod behaviors under irradiation conditions caused by burnup  
 140 degradation, swelling, expansion, creep and stress-strain are  
 141 accurately simulated and the evolution of intra-pellet temper-  
 142 ature distribution with burnup is generated.

143 It is worthy emphasizing that unlike most deterministic di-  
 144 rect whole core calculation codes that runs on CPU-based  
 145 dedicated supercomputers, CRANE by design is a fully-  
 146 GPU-based code and its target computing platform is cho-  
 147 sen as industry-affordable computer server mounted with 10  
 148 consumer-grade GPUs. As depicted below in Fig. 1 the flow  
 149 chart of CRANE, where modules marked in green runs on  
 150 GPU and modules marked in blue runs on CPU, it can be con-  
 151 cluded that for CRANE almost all the computation-related  
 152 modules run on GPU, only these modules that are performed  
 153 only for once, such as input parsing, cross-section data li-  
 154 brary reading, geometric processing, and result editing, run  
 155 on CPU. Moreover, in order to fully exploit the GPU comput-  
 156 ing power, the algorithms related to neutronics and thermal-  
 157 hydraulics have been carefully designed for the GPU architec-  
 158 ture, and extensive performance optimizations have been per-  
 159 formed to ensure high parallel efficiency and the efficient use  
 160 of limited GPU memories. For instance, to fully exploit the  
 161 GPU computing power, long characteristic ray tracing rather  
 162 than the cyclic characteristic ray tracing is adopted in CRANE  
 163 and the 1D thermal conduction calculation for each axial node  
 164 of all the fuel rods are solved in batches on GPU, with one  
 165 GPU thread handling the computation of one node.

166 Moreover, in order to achieve high efficiency in multi-  
 167 physics coupling iterations, CRANE utilizes direct shared  
 168 memory for data exchange and adopts a unified mesh sys-  
 169 tem for modeling, which makes the data exchange between

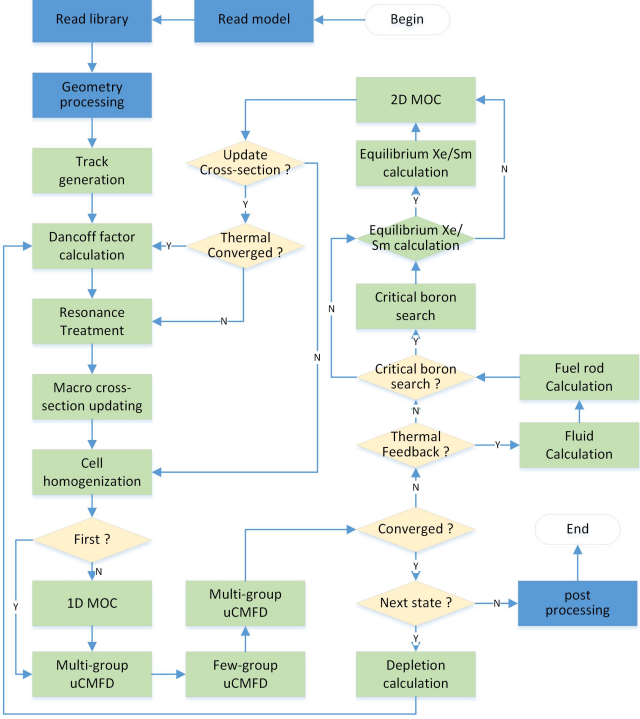


Fig. 1. Flow chart of CRANE

170 different modules extremely fast and eliminates the need to  
 171 perform mesh and data mapping between different modules.  
 172 This kind of highly-integrated coupling between neutronics  
 173 and thermal-hydraulic modules further guarantee the excep-  
 174 tional computational speed performance of CRANE.

175

### III. CORE MODELING

176 The reactor core specified in the BEAVRS benchmark  
 177 problem is a four-loop Westinghouse PWR loaded with 193  
 178 optimized fuel assemblies of  $17 \times 17$  lattice for the rated  
 179 power of 3411 MWth. The benchmark specification pro-  
 180 vides all the detailed geometric dimensions and the material  
 181 compositions for the major core constituents including fuel  
 182 assemblies with different fuel enrichment, borosilicate glass  
 183 burnable absorber, control rods, core baffle and barrel.

184 As the first step of the benchmark calculation, a virtual  
 185 core model that faithfully represents the practical core is set  
 186 up. Since CRANE employs Constructive Solid Geometry  
 187 (CSG) method for modeling in the x-y plane, it is capable of  
 188 faithfully modeling all the geometrical details of the problem  
 189 without introducing any approximations. Fig. 2 and Fig. 3  
 190 show the core model that CRANE outputted by exploiting the  
 191 Python visualization tool package.

192 More detailed information about CRANE BEAVRS core  
 193 modeling is given as follows:

- 194 In the radial direction, the 1/4 symmetric core is mod-  
 195 eled, with the outer boundary setting at one fuel as-  
 196 sembly width outside the active core; while in the ax-

ial direction, the code automatically generates the axial meshes according to the material heterogeneity with the maximum height of an axial layer setting to be 20 cm. In the end, the whole height of the problem is divided into 38 layers, of which 29 layers are in the active core. There are 9 spacer grids in total along the height, each height containing the spacing grid is set as a separate layer and all the spacer grid strap in these layers are explicitly modeled.

- 206 In terms of spatial mesh division for the neutronics calcu-  
 207 lation, Fig. 4(a) and (b) show the flat source approxi-  
 208 mation mesh division schemes that CRANE adopted  
 209 for a normal fuel pin cell and a burnable absorber pin  
 210 cell respectively.
- 211 The ray tracing parameters used for MOC calculation  
 212 are as follows: for the radial 2D MOC calculation, the  
 213 Tabuchi-Yamamoto optimum polar angle quadrature  
 214 set[14] is employed, using 3 polar angles and 12 azi-  
 215 muthal angles for the octant of the solid angle sphere,  
 216 and 0.05 cm ray spacing; while for the axial 1D MOC  
 217 calculation, the Legendre quadrature set is employed,  
 218 using 8 discrete angles in the range of  $0-\pi$  and 0.5 cm  
 219 mesh height for flat source approximation.
- 220 Pin-wise thermal hydraulics (T/H) feedback is consid-  
 221 ered by solving the corresponding model for coolant  
 222 and fuel rod, however, only the simple closed channel  
 223 T/H module was used instead of the more time consum-  
 224 ing elaborated sub-channel module since the cross flow  
 225 between adjacent pin cells is small and has a negligible  
 226 effect on core reactivity and power distributions.
- 227 Convergence criteria: The criterion for critical boron  
 228 concentration search is 0.5 ppm, the convergence crite-  
 229 rion for calculating control rod worth and temperature  
 230 coefficient is 0.2 pcm for k-effective, the convergence  
 231 criterion for fission source is  $5 \times 10^{-4}$ , and the conver-  
 232 gence criteria for T/H feedback calculations are 0.2 K  
 233 for coolant temperature and 1 K for fuel pellet temper-  
 234 ature respectively.

### IV. VALIDATION RESULTS

#### 1. HZP core calculation of Cycle 1

235 Table 1 shows the critical boron concentrations calculated  
 236 by CRANE under 5 different control rod insertion states at  
 237 the beginning of the Cycle 1 (BOC1) and the corresponding  
 238 deviation from the measurements. The maximum deviation  
 239 is 25 ppm, which meets well the requirement of American  
 240 Nuclear Society (ANS) standards[15], i.e., the deviations be-  
 241 tween measured value and predicted value should be less than  
 242  $\pm 50$  ppm. Reference[16] gives the standard deviation of the  
 243 measured critical boron concentration, which is 22 ppm for  
 244 all the 5 measurements. It can be seen that except for the

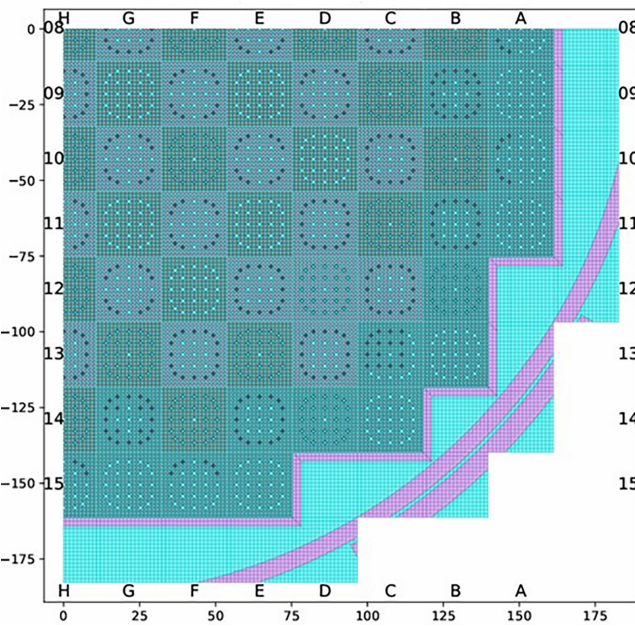


Fig. 2. Radial modeling of BEAVRS core

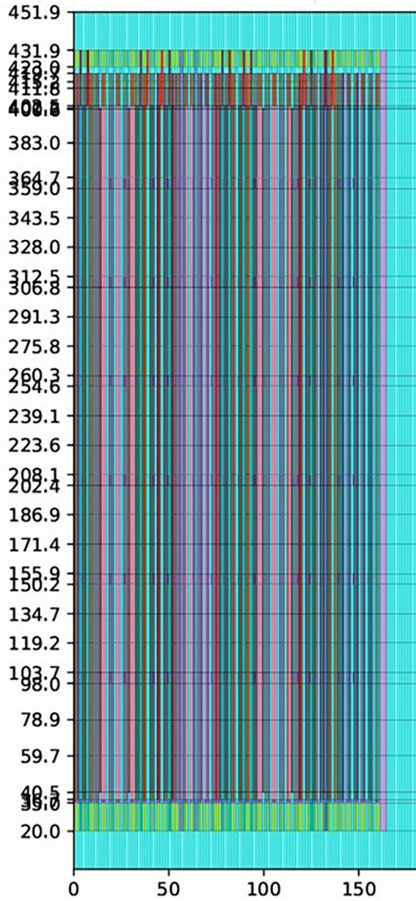


Fig. 3. Axial modeling of BEAVRS core

D-in state, where the deviation slightly exceeds the standard deviation of the measurements, all the other 4 deviations lie well within the range of the standard deviation of the measurement.

Moreover, since the variation in critical boron concentration under different control rod insertion states directly reflects the control rod worth. From the results in this table, it can also be inferred that all prediction deviations of control rod worth characterized by boron concentration variations fall within the range of standard deviation of the boron concentration measurements.

To compare the prediction accuracy of CRANE with that of relevant codes in the world, Table 1 also presents the prediction deviation of the deterministic code VERA[17] and Monte Carlo code RMC[18]. The accuracy of CRANE for criticality prediction is fully comparable to that of VERA and RMC.

Table 2 shows the validation results of CRANE control rod worth prediction. The maximum relative deviation for the worth of individual bank is -10%, and the deviation for the total integral of predicted worths is -1.5%. The CRANE prediction accuracy meets the requirements of the ANS standards[15], i.e. the deviation for the worth of individual bank should be within  $\pm 15\%$  or 100 pcm, whichever is greater, and the deviation for the total integral of control rod worths should be within  $\pm 10\%$  (for Dynamic Rod Worth Measurement, the total worth should be within 8%).

Similar to the comparison of the critical boron concentration, Table 2 also presents the prediction deviation of code VERA and RMC. In general, the prediction accuracy of CRANE is comparable to that of VERA and RMC. Moreover, when comparing the prediction deviation of each rod bank, it can be noticed that in all the three groups of deviations, the deviations of rod bank A and SE are relatively or exceptionally larger. It is believed that this is mainly caused by the relatively larger errors in the measured values for these two rod banks.

Table 3 shows the validation results for isothermal temperature coefficient (ITC). The benchmark problem gives 3 measured values at different control rod insertion states. For each core state, the CRANE prediction meets well the ANS standard requirements, i.e. the deviation should be less than  $\pm 2\text{ pcm}/^{\circ}\text{F}$ .

## 2. Core follow calculation of Cycle 1

Fig. 5 gives the detailed power operation history of the initial cycle of BEAVRS problem, where the blue dots denote the time that the in-core neutron flux measurements is carried out. There are in total 24 in-core measurements performed during the whole cycle. For each in-core measurement, the benchmark problem provides detailed core state information, as well as the movable detector signals obtained from the fifty-eight instrumented assemblies. In addition, the benchmark problem also provides the boron letdown data at 29 different equivalent full power days (EFPD).

In order to validate the core depletion characteristics against the measured data, the core follow calculations were

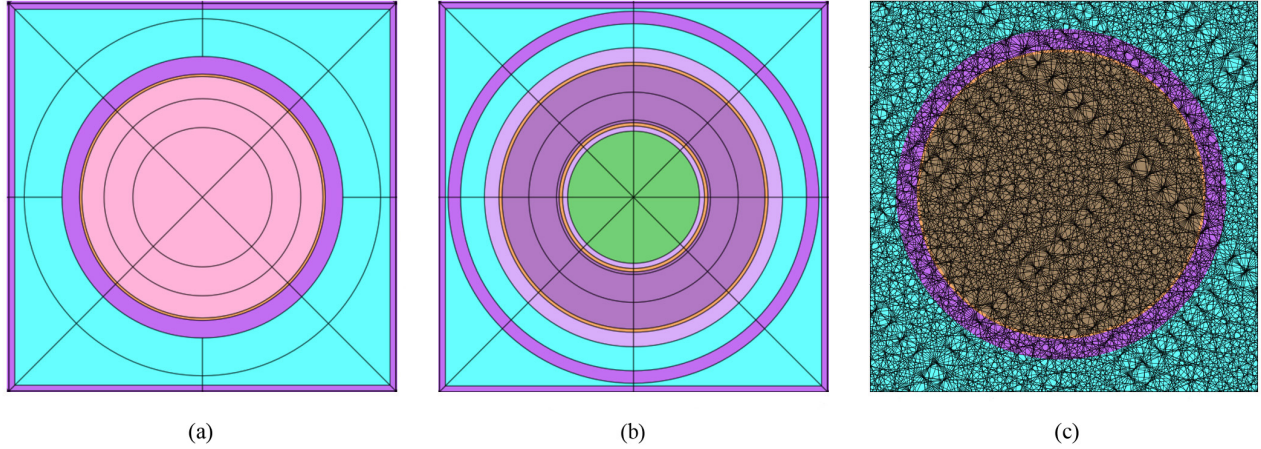


Fig. 4. (a) Fine mesh of fuel pin. (b) Fine mesh of burnable poison rod. (c) 2D-MOC track.

Table 1. Comparisons of BOC1 HZP critical boron concentrations

Case	CBC[ppm]	Std. Dev.[ppm]	CRANE[ppm]	$\Delta$ CRANE[ppm]	$\Delta$ VERA[ppm]	$\Delta$ RMC[ppm]
ARO	975	22	988	13	1	-14
D in	902	22	927	25	13	-4
C, D in	810	22	833	23	4	-9
A, B, C, D in	686	22	698	12	-5	-25
A, B, C, D, SE, SD, SC in	508	22	513	5	-16	-39

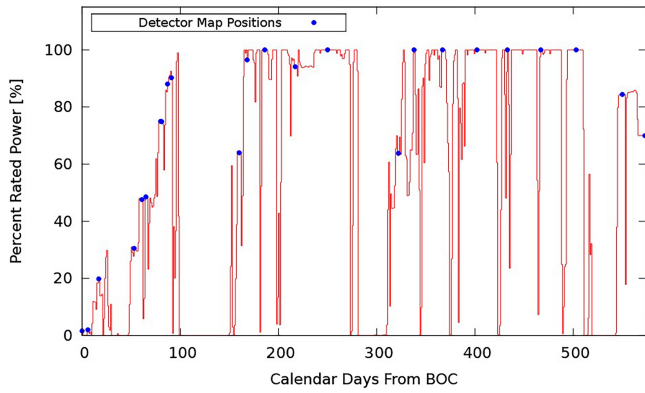


Fig. 5. Power history of Cycle 1

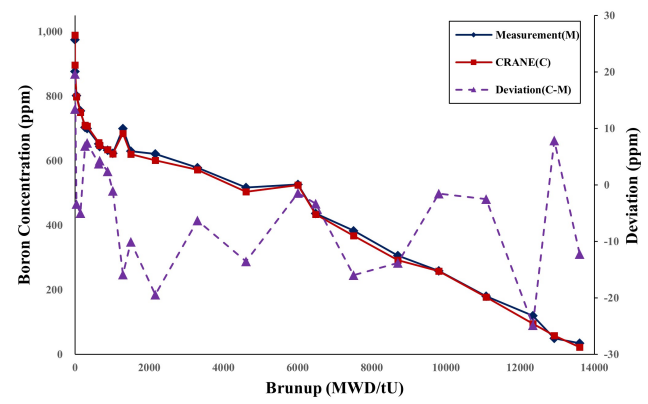


Fig. 6. Comparison of core follow critical boron concentration with measured data for Cycle 1

302 performed for the initial cycle of the BEAVRS core. The  
 303 uniqueness of this work is that it adopts the exact power his-  
 304 tory to perform core follow calculation, since today's GPU  
 305 computing power enables CRANE to do so. While for most  
 306 existing CPU-based high-fidelity codes, people usually have  
 307 to adopt simplified or approximated power history to com-  
 308 plete the BEAVRS Cycle 1 core follow calculation. Because  
 309 the large computational cost required for exactly tracking the  
 310 complex power history makes it impractical for these codes  
 311 to do so.

312 Fig. 6 gives the comparison of critical boron concentrations  
 313 obtained from the core follow calculation with these specified

314 by the problem for 24 different burnup states, where the in-  
 315 core flux measurement is carried out. The CRANE prediction  
 316 agrees well with the measurement and the deviations through-  
 317 out the entire cycle are generally less than  $\pm 25$  ppm.

318 The benchmark problem provides the reference boron let-  
 319 down data for Cycle 1. In order to perform the boron letdown  
 320 curve comparison, one has to obtain the critical boron concen-  
 321 tration under the standard boron condition, i.e. the concen-  
 322 tration under the all-rod -out (ARO) and hot-full-power(HFP)  
 323 state. Although with the previous core follow boron concen-  
 324 tration results available, one may obtain this boron concen-

Table 2. Comparisons of BOC1 HZP Control Rod Worths

Bank	CRW [pcm]	Std. Dev. [pcm]	Error[%]	CRANE[pcm]	$\Delta$ CRANE[%]	$\Delta$ VERA[%]	$\Delta$ RMC[%]
D	788	29	3.6	775	-1.6	-1.1	1.3
C	1203	32	2.6	1175	-2.3	4.2	2.5
B	1171	31	2.7	1247	6.5	2.1	-2.0
A	548	26	4.8	493	-10.0	5.7	-9.5
SE	461	25	5.5	416	-9.8	5.9	-3.0
SD	772	28	3.7	762	-1.3	0.9	3.4
SC	1099	31	2.8	1082	-1.5	-0.1	3.5
Total	6042	-	-	5950	-1.5	2.2	0.7

Table 3. Comparisons of BOC1 HZP Isothermal Temperature Coefficients

Case	ITC[pcm/ $^{\circ}$ F]	Std. Dev. [pcm/ $^{\circ}$ F]	CRANE[pcm/ $^{\circ}$ F]	$\Delta$ CRANE[pcm/ $^{\circ}$ F]	$\Delta$ VERA[pcm/ $^{\circ}$ F]	$\Delta$ RMC[pcm/ $^{\circ}$ F]
ARO	-1.75	0.54	-2.64	-0.89	-0.81	-0.53
D in	-2.75	0.54	-3.96	-1.21	-1.26	-0.80
C, D in	-8.01	0.54	-8.57	-0.56	-0.79	-0.04

tration by introducing theoretical corrections to consider the power and control rod effects, in this study, more straightforward method is applied, i.e. directly perform ARO HFP depletion calculation for Cycle 1. Fig. 7 shows the obtained results with the reference ones where the non-physical minus boron concentration at the end of cycle in the predicted value is because of that the predicted cycle length is slightly shorter than the reference one. One may notice that for the whole core lifetime of Cycle 1, the deviation of standard boron concentration lies within the range of  $\pm 25$  ppm, which is consistent with the above-mentioned core follow calculation results. As a supplement, Fig. 7 also shows the boron letdown curve predicted by the nTRACER[19] code, the results of CRANE and nTRACER are also in good agreement. Both CRANE and nTRACER slightly under-estimate the cycle-length of Cycle 1 and the situation of CRANE is slight better than that of nTRACER.

Reference [16] investigated the uncertainty of BEAVRS boron concentration measurement by analyzing the results of multiple measurements of boron concentration in the same day and comparing the deviation between the measured value and the calculation result of the analysis code currently used in engineering, and the conclusion was that the uncertainty is  $\pm 25$  ppm, which is entirely consistent with the deviations that one may observe in Fig. 6 and Fig. 7. Therefore, it is concluded that CRANE is able to accurately predict the BEAVRS core reactivity variation for the entire lifetime of Cycle 1.

### 3. In-core detector signal calculation of Cycle 1

In this subsection, the accuracy of CRANE in calculating the 3D neutron flux distribution within the reactor core is validated against the in-core flux measurements provided by the BEAVRS benchmark problem. Since what the bench-

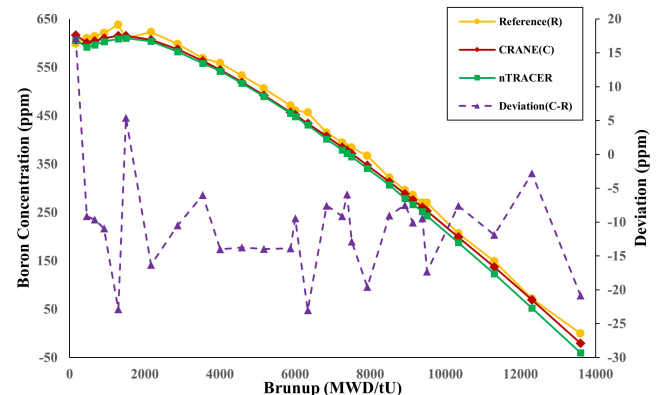


Fig. 7. Comparison of boron letdown curves in the Cycle 1 standard boron state

mark problem provided is just the normalized 3D detector response, not the detector current signal itself, the in-core detector signal is simulated in this study by putting a trace amount of U-235 in the instrumentation thimble to generate the fission rates at all the detector locations. The resulting detector fission rates are then normalized to generate a 3D distribution that can be compared with the measured 3D detector response.

As shown in Fig. 5, many in-core flux measurements of Cycle 1 were carried out during the power ascension process. The change of power level will cause the delayed change of xenon spatial distribution in the reactor, which will lead to the change of neutron flux distribution. Such transient fluctuations cannot be accurately calculated according to the operation history in days given by the benchmark. Therefore, just like the practice adopted in reference[17], only 14 sets of measurement data obtained at relative high-power level and

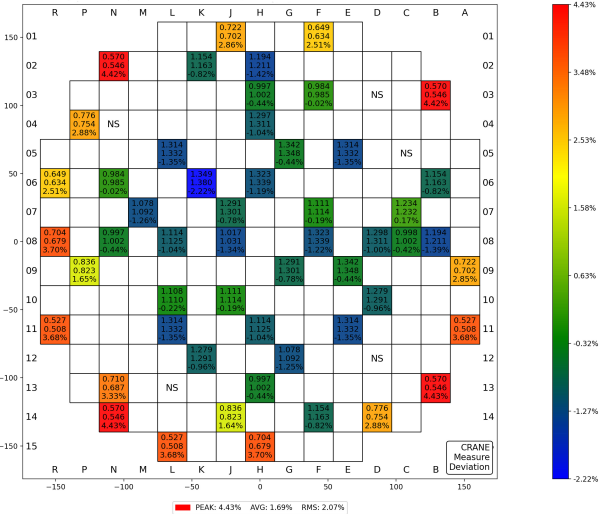


Fig. 8. Cycle 1 1295.50 MWdtU 64%FP detector signals relative difference

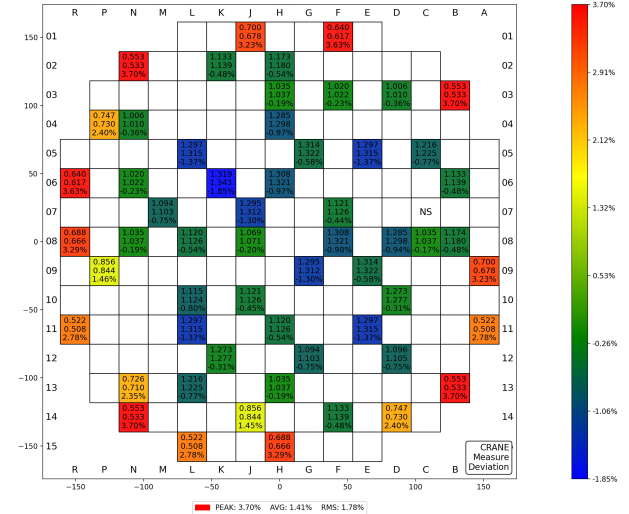


Fig. 9. Cycle 1 4613.50 MWdtU 100%FP detector signals relative difference

have been relatively stable are selected to be compared with. The comparison results are summarized in Table 4, where 2D RMS means the root mean square deviation between the predicted and measured 2D detector signal distributions. The 2D predicted and measured distributions are obtained by integrating the corresponding 3D detector signal distributions in the axial direction. The comparison given in Table 4 indicates that the accuracy of in-core detector signal prediction at different burnup for both CRANE and VERA are basically comparable.

To learn more detailed about the deviations in the detector signal distribution, Fig. 8- 10 each present a two-dimensional detector signal distribution deviation at a specific burnup point for the beginning, middle, and end of the cycle. From these comparisons, it can be seen that in general the accuracy of CRANE prediction is satisfactory, with the maximum relative deviation less than 5%. However, it can also be observed that compared to the measured signals, the signals predicted by CRANE exhibit a slight in- and out-ward tilt and the tilt decreases as the fuel burnup feedback increases.

#### 4. HZP core calculation of Cycle 2

At the beginning of Cycle 1, all the fuel loaded into the core are fresh fuels. For Cycle 2, which is a reloaded core, there are both depleted fuels and also fresh fuels loaded into the core at the beginning of the cycle. Engineering functions such as deplete fuel shuffling and removing the borosilicate glass burnable absorber rod from the deplete fuel from Cycle 1 are necessary for a code to perform Cycle 2 calculations. Therefore, the Cycle 2 problem provides not only a case to further validate the core depletion functionality of a core analysis code but also a good benchmark to check whether the code possesses the necessary functionality such as fuel shuffling for engineering applications.

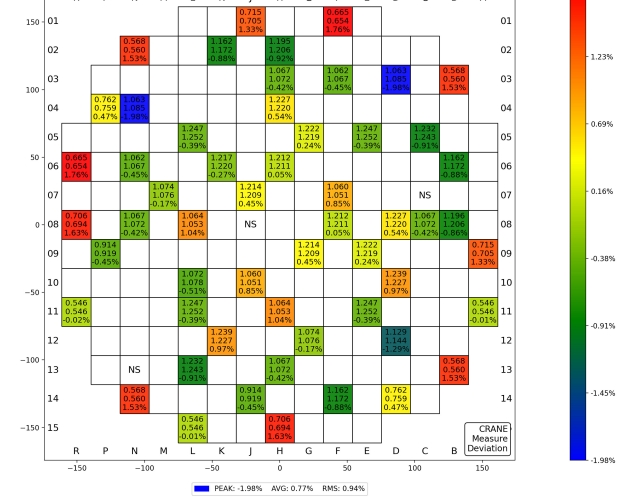


Fig. 10. Cycle 1 12341.20 MWdtU 100%FP detector signals relative difference

The CRANE code was adopted to perform HZP core calculation of Cycle 2 of BEAVRS problem. Critical boron concentration, isothermal temperature coefficient, control rod worth corresponding to the measurement were predicted and the comparison results are summarized in Table 5 and Table 6 respectively. It can be seen that the predicted critical boron concentration and temperature coefficient are in good agreement with the measurement, and the degree of deviation between the prediction and measurement is similar to that of the first cycle. Meanwhile, it can also be seen that CRANE and VERA have comparable prediction accuracy for criticality calculation.

When looking at the validation results of CRANE control rod worth prediction, it is noticed that in general the prediction accuracy is similar to that of the first cycle and meets the

Table 4. Comparison of 2D detector signal distributions at different burnup of Cycle 1

Depletion [MWD/tU]	Power [%]	CRANE 2D RMS [%]	VERA 2D RMS [%]
1023	99	2.02	1.67
1296	64	2.07	3.42
1507	100	2.52	0.84
2163	100	2.73	1.18
3297	94	1.92	0.82
4614	100	1.78	0.90
6012	64	1.11	1.18
6490	100	1.90	1.23
7508	100	1.22	0.88
8701	100	1.12	0.99
9803	100	1.15	3.24
11084	100	1.06	1.12
12343	100	0.94	1.21
12915	84	1.38	1.48
Cycle average	-	1.75	1.46

422 requirements of the ANS standard. However, unlike the first  
423 cycle, there are more banks of rod with deviations reaching  
424 around 10%, and the maximum relative deviation has reached  
425 12.7%. The reason for this phenomenon, as believed in this  
426 study, is mainly due to the errors in the measurements them-  
427 selves. Looking at the standard deviation errors of measure-  
428 ment given in Table 6 and Table 2, it can be found that the  
429 error is further increased at Cycle 2, especially for banks with  
430 relative small control rod worth, such as bank SD, SC and SA,  
431 where the measurement error itself exceeds 7%.

432 As mentioned earlier there is no existing literature pub-  
433 lished the control rod worth prediction for Cycle 2 of  
434 BEAVRS problem, therefore there is no validation results of  
435 other code provided in Table 6.

436

### 5. Core follow calculation of Cycle 2

437 As the practice of the Cycle 1, Cycle 2 core follow cal-  
438 culation adopting the exact power history depicted in Fig 11  
439 was performed, and the CRANE predicted boron concentra-  
440 tions were compared against the measurements specified for  
441 14 burnup states where the in-core flux measurement is car-  
442 ried out. Moreover, ARO HFP core depletion calculations  
443 were also performed and the obtained boron concentrations  
444 were compared against the reference boron letdown data as  
445 well as the ones predicted by the nTRACER code. Compar-  
446 ison results are shown in Fig 12 and Fig 13 respectively. It  
447 can be seen that except for one isolated instance of core fol-  
448 low calculation where the deviation of boron concentration  
449 exceeds 35ppm, all the other deviations between the CRANE-  
450 predicted and the measured critical boron concentration for  
451 both core follow calculation and boron letdown curve calcu-  
452 lation are less than 25 ppm throughout the entire cycle. Con-

453 sidering that the uncertainty of BEAVRS boron concentration  
454 measurement is  $\pm 25$  ppm, once again, one may conclude that  
455 CRANE is able to predict the BEAVRS core reactivity varia-  
456 tion for the reload cycle with satisfying accuracy. The com-  
457 parable accuracy between CRANE and nTRACER results is  
458 also demonstrated.

### 459 6. In-core detector signal calculation of Cycle 2

460 For Cycle 2, there are in total 14 in-core flux measure-  
461 ments performed during the whole cycle, and all these measure-  
462 ments are simulated by CRANE. The obtained 2D in-core de-  
463 tector signal distributions are compared against the measure-  
464 ments and the results are summarized in Table 7. To facilitate  
465 the performance assessment between CRANE and other high-  
466 fidelity codes, the in-core detector signal validations results  
467 of the deterministic code VERA and the Monte Carlo and

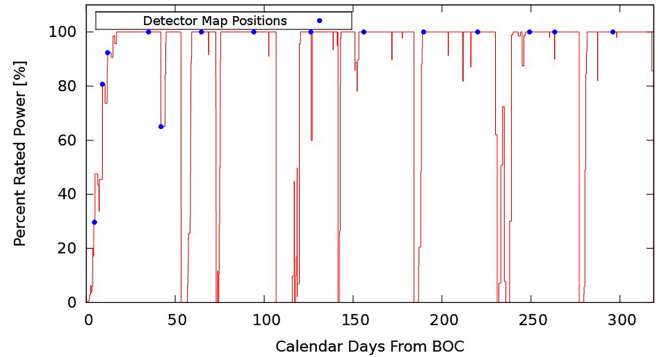


Fig. 11. Power history of Cycle 2

Table 5. Comparisons of Cycle 2 Critical Boron Concentrations and Isothermal Temperature Coefficient

Test type	Case	Measurement	Std. Dev.	CRANE	$\Delta$ CRANE	$\Delta$ VERA
CBC [ppm]	ARO	1405	22	1401	-4	-8.6
CBC [ppm]	C in	1273	22	1300	27	21.4
ITC [pcm/ $^{\circ}$ F]	ARO	1.71	0.54	1.27	-0.44	-

Table 6. Comparisons of Cycle 2 Control Rod Worth

Bank	Measurement[pcm]	Std. Dev.[pcm]	Error[%]	CRANE [pcm]	$\Delta$ CRANE[%]
D	426	25	5.8	470	10.21
C	1014	30	3.0	1028	1.34
B	716	28	3.9	705	-1.60
A	420	25	5.9	408	-2.75
SE	438	25	5.7	445	1.56
SD	305	23	7.5	344	12.69
SC	307	23	7.5	336	9.44
SB	781	29	3.6	793	1.54
SA	326	23	7.1	356	9.06
Total	4733	-	-	4883	3.17

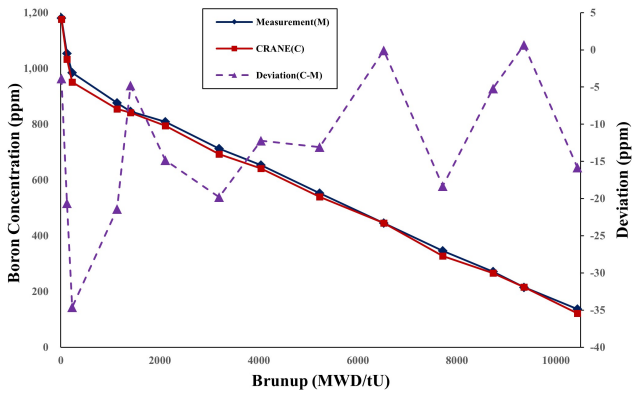


Fig. 12. Comparison of measured boron concentration and CRANE results in Cycle 2

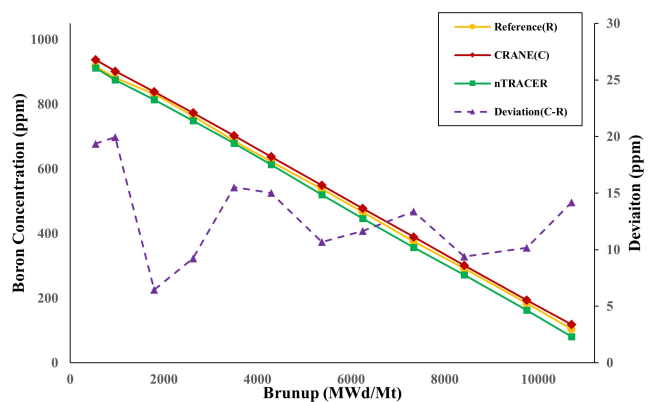


Fig. 13. Comparison of boron letdown curves in the Cycle 2 standard boron state

468 thermal hydraulics code coupled system (MCS+CTF)[20] are  
469 also provided in Table 7. Based on these comparison results,  
470 it can be concluded that CRANE is able to accurately predict  
471 the in-core flux distribution and its variation with fuel burnup  
472 for the whole cycle. The accuracy of CRANE to predict the  
473 in-core detector signal is fully comparable to that of VERA,  
474 and generally better than the MCS/CTF system. Neverthe-  
475 less, unlike the VERA case where the RMS error at the first  
476 two burnup points are evidently larger, the error of CRANE  
477 is rather stable throughout the cycle.

478 As the practice of Cycle 1, three representative detector  
479 signal deviation distributions are shown in Fig. 14 to Fig. 16.  
480 Compared with the ones for Cycle 1, the results of Cycle 2 are  
481 overall better, the relative deviation of all the results is within

482 5% and the in- and out-ward tilt existed in the deviation dis-  
483 tribution for Cycle 1 are no longer existed for this cycle.

## 484 V. SPEED PERFORMANCE AND POTENTIAL FOR 485 PRACTICAL APPLICATIONS

486 As the core analysis method shifts from the conventional  
487 two-step procedure to the direct whole core calculation in-  
488 volving first-principle-based simulations of the multi-physics  
489 behaviors in nuclear reactors, the computation load increases  
490 significantly. It is estimated that the computation load of the  
491 new method is at least 2 to 3 orders of magnitude greater than  
492 that of the conventional method. Desktop personal computer  
493 or workstation, which are the computing platform for the con-

Table 7. Cycle 2 deviation of detector signals under different burnup

Depletion [MWD/tU]	Power [%]	CRANE 2D RMS [%]	VERA 2D RMS [%]	MCS+CTF 2D RMS [%]
12.92	29	1.67	3.11	4.08
125.45	80	1.22	3.22	2.43
224.65	100	1.42	1.57	2.90
1126.14	100	1.06	1.11	3.10
1395.39	65	1.48	-	2.99
2091.83	100	1.04	1.04	2.90
3169.63	100	1.04	1.15	2.70
4006.52	100	1.19	1.14	2.65
5178.51	100	1.14	1.12	1.47
6463.87	100	1.31	1.18	2.59
7645.03	100	1.40	1.38	3.03
8650.31	100	1.18	0.95	2.81
9272.15	100	1.17	1.16	3.11
10338.69	100	1.04	1.11	1.17
Cycle average	-	1.26	1.43	2.71

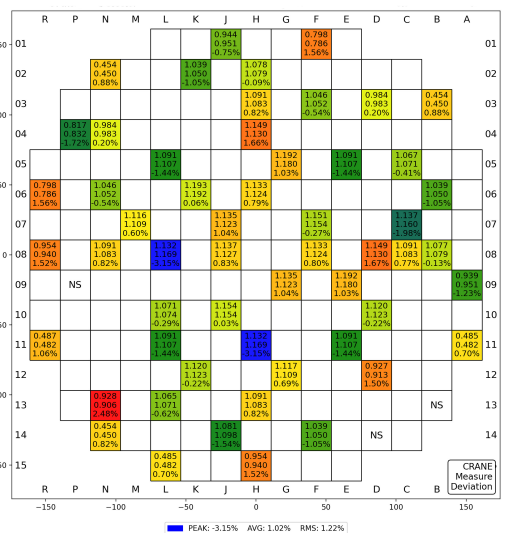


Fig. 14. Cycle 2 125.45 MWdtU 80%FP detector signals relative difference

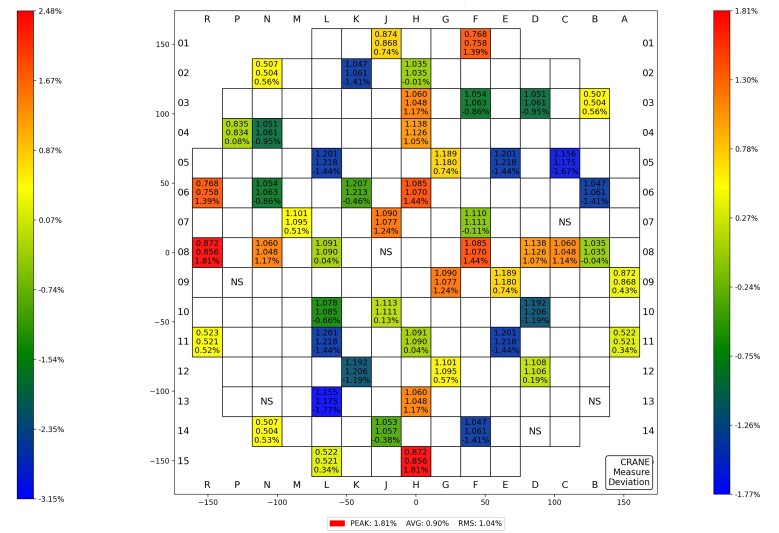


Fig. 15. Cycle 2 3169.63 MWdtU 100%FP detector signals relative difference

494 conventional method, are no longer suitable for the new method  
495 due to their limited computing power and memories. High-  
496 performance computing (HPC) clusters or supercomputers  
497 equipped with many CPUs are chosen by many institutions  
498 in the world as the computing platform for the new genera-  
499 tion PWR core analysis codes. However, due to the complex-  
500 ity of the problem, even by exploiting the computing power  
501 of today's HPC clusters or supercomputers, it is still a chal-  
502 lenging task to reduce the computing time of the direct whole  
503 core calculation code to a practical level such that it can be  
504 used in routine design analysis. For instance, to simulate the  
505 BEAVRS benchmark, VERA takes 50min (760 CPU-hrs) on

506 average to complete the corresponding one state core analysis  
507 on a cluster with 880 2.3 GHz Intel Xeon processors with 4  
508 GB RAM [17]; while nTRACER takes 3 hours for a single-  
509 step calculation running on a cluster with 28 computing nodes  
510 mounted with dual 2.67 GHz INTEL XEON X5650 proces-  
511 sors yielding 12 cores per node[19].

512 Moreover, as can be deduced from the above-mentioned  
513 VERA and nTRACER results, in order to reduce the com-  
514 puting time of a new generation code to a practical level,  
515 supercomputers mounted with thousands of cores are neces-  
516 sary. Unfortunately, such large-scale HPC clusters are usually  
517 available only at national laboratories, not at nuclear design

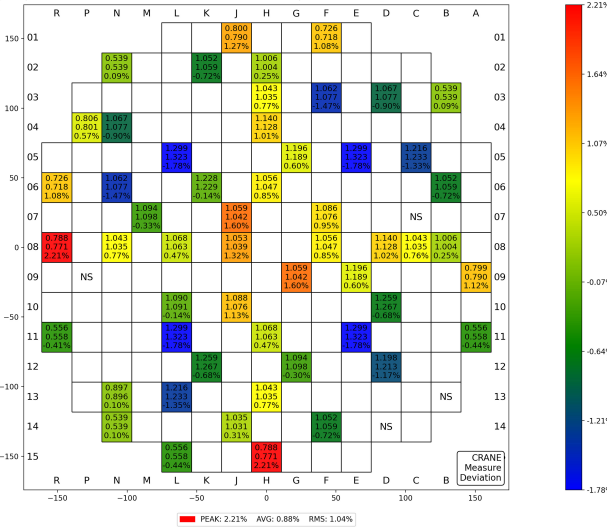


Fig. 16. Cycle 2 10338.69 MWdtU 100%FP detector signals relative difference

518 institutes, not to say ordinary research groups. Therefore,  
 519 both the computing time and the platform availability issue  
 520 pose a key obstacle that hinders the widespread use of these  
 521 new generation codes based on HPC cluster or supercomputer  
 522 based.

523 Meanwhile, in the past two decades, the computing power  
 524 of GPUs has exhibited a much stronger growth than that of  
 525 CPUs. The computing power that used to be provided by  
 526 multiple CPU nodes can now be provided by a single GPU  
 527 card. GPUs provide much higher computing power than  
 528 CPUs for the same energy consumption. It thus provides the  
 529 researchers a new platform to consider for the development of  
 530 the direct whole core calculation codes for PWRs, i.e. adopting  
 531 heterogeneous computing that utilizes more GPUs than  
 532 CPUs. In this regard, the Reactor Physics Lab of Seoul Na-  
 533 tional University has conducted valuable exploration[21][22].  
 534 It is demonstrated that after proper porting the legacy CPU  
 535 code to GPU, significant speedup can be achieved for an  
 536 industrially affordable GPU-based heterogeneous computing  
 537 platform mounted with consumer-grade GPUs.

538 In this study, the BEAVRS benchmark problem is solved  
 539 using the CRANE code. One of the uniqueness of CRANE  
 540 is that it is by design a fully-GPU-based code. As depicted  
 541 in the flow chart of CRANE (Fig 1), for CRANE, the GPU  
 542 computing is not just for acceleration, but the main force  
 543 of the computation, since almost all the computation-related  
 544 modules run on GPUs. To resolve the above-mentioned is-  
 545 sue of platform availability, the target computing platform  
 546 of CRANE is chosen as industry-affordable computer server  
 547 mounted with consumer-grade GPUs. All calculations for  
 548 this work are completed on a small server equipped with 10  
 549 RTX 3090 graphics cards, and the peak power consumption  
 550 of the server is 4kW. The statistics indicates that to complete  
 551 all the validations for the parameters specified in BEAVRS  
 552 benchmark, 738 different core states were analyzed and it  
 553 took 15.7 hours in total. The average time needed to complete

554 one state multi-physics coupled high-fidelity core analysis is  
 555 63.5s and 101.2s respectively for cycle 1 and cycle2.

556 This speed performance is significant because it fully  
 557 demonstrates the power of GPU computing, which is that  
 558 it can reduce the time required to complete a high-fidelity  
 559 simulation of a large commercial pressurized water reactor  
 560 to the minute level, without resorting to dedicated supercom-  
 561 puters, but merely by using low-cost consumer-grade graph-  
 562 ics cards. A summary of the key computation conditions and  
 563 corresponding speed performances employed by several di-  
 564 rect whole core calculation codes for the BEAVRS bench-  
 565 mark problem is presented in Table 8. The data in the table  
 566 reveals that the outstanding speed performance of CRANE is  
 567 achieved by using more energy groups and more axial layers  
 568 than other codes.

569 Another advantage of developing the new generation code  
 570 based on the CPU-GPU heterogeneous platform is the ability  
 571 to continuously leverage the rapidly advancing GPU technol-  
 572 ogy to enhance the computational speed of the code. The  
 573 RTX 3090 graphics card used in this paper for the BEAVRS  
 574 problem computation was released in 2020, and since then,  
 575 NVIDIA company has successively released the RTX 4090  
 576 and 5090 graphics cards with superior performance. The au-  
 577 thor ever had a chance to run the CRANE code on another  
 578 platform equipped with RTX 4090 GPUs, and the new com-  
 579 putation time is just about 50-60% of that for the current 3090  
 580 platform, i.e., the high-fidelity calculation of a single core  
 581 state of a large commercial reactor, which currently takes  
 582 1-2 minutes to complete, can basically be finished within 1  
 583 minute on the new 4090 platform. Considering the rapid in-  
 584 crease in the performance of GPU graphics cards, the author  
 585 believes that more and more computation-extensive CPU-  
 586 based legacy codes will be ported to the GPU-CPU heteroge-  
 587 neous platform, and CRANE, as a fully GPU-based pioneer  
 588 code, will have a good chance to be widely used as a routine  
 589 tool in the nuclear power industry.

## VI. CONCLUSION

591 The BEAVRS benchmark problem has been successfully  
 592 analyzed with the CRANE code, which is a fully GPU-based  
 593 deterministic direct whole core calculation code targeted for  
 594 PWR practical applications. Detailed reactor core models are  
 595 set up, which faithfully represent the practical core of the  
 596 initial two cycles. Core follow calculations are performed  
 597 by adopting the exact power history of the reactor. Vali-  
 598 dation against all the measurement data shows that the pre-  
 599 dicted criticality, control rod bank worths, in-core detector  
 600 signal distribution and the boron let-down curves of two cy-  
 601 cles agree well with the measurements. The deviations of the  
 602 predicted results are all within the acceptable range for en-  
 603 gineering applications. Moreover, it is demonstrated that by  
 604 fully exploiting the GPU computing power, direct whole core  
 605 calculation without resorting to the dedicated supercomputer  
 606 mounted with thousands of cores is possible. Direct whole  
 607 core calculation with detailed core model can be realized on  
 608 an industry-affordable mini computer server mounted with 10

Table 8. Summary of calculation conditions and speed performance for different codes

Code	CRANE	VERA[17]	nTRACER[22]	nTRACER[22]
Platform	Intel Xeon Platinum 8375C CPU, 64 cores with 1 TB RAM, 10 RTX 3090	Intel Xeon 2.3 GHz CPU, 880 cores with 4 GB RAM	Intel Xeon E5-2640 v3 CPU, 288 cores with 128 GB RAM,	Intel Xeon E5-2630 v4 CPU, 180 cores with 256 GB RAM, 36 RTX 2080
# of Energy groups	69	51	47	47
# axial planes	38	34	36	36
Execution time per core state	1~2min	50min	2.1h	15min

609 consumer-grade RTX 3090 graphics cards, and the average 612 These results indicate that CRANE possesses high solution fi-  
 610 time needed to complete multi-physics coupled high-fidelity 613 delity and superior speed performance, it has good prospects  
 611 analysis for single core state point is just about one minute. 614 for PWR engineering applications.

615 [1] Joo, H.G., Cho, J.Y., Kim, K.S. *et al*, Methods and Perfor- 617 mance of a Three-Dimensional Whole-Core Transport Code 618 DeCART. International Conference on Physics of Reactors 619 (PHYSOR 2004); 2004 Apr 25–29; Chicago, IL.

620 [2] Jung, Y.S., Shim, C.B., Lim, C.H. *et al*, Practical numeri- 621 cal reactor employing direct whole core neutron transport and 622 subchannel thermal/hydraulic solvers. *Ann. Nucl. Energy* 62, 623 357–374. (2013) DOI:10.1016/j.anucene.2013.06.031

624 [3] Kochunas, B., Collins, B., Martin, W.R. *et al*, Overview of 625 Development and design of MPACT: Michigan parallel char- 626 acteristics transport code. *Intl. Conf. Mathematics and Com- 627 putational Methods Applied to Nuclear Science & Technology* 628 (M&C 2013); 2013 May 5–9; Sun Valley.

629 [4] Chen, J., Liu Z., Zhao, C. *et al*, A new high-fidelity neutron- 630 ics code NECP-X. *Ann. Nucl. Energy* 116, 417–428. (2018) 631 DOI:10.1016/j.anucene.2018.02.049

632 [5] Sutton, T.M., Tj, D., Trumbull, T. *et al*, The MC21 Monte Carlo 633 Transport Code. Joint International Topical Meeting on Mathe- 634 matics and Computations and Supercomputing in Nuclear Ap- 635 plications.(2007)

636 [6] Wang, K., Li, Z., She, D. *et al*, RMC – A Monte Carlo code for 637 reactor core analysis. *Ann. Nucl. Energy* 82, 121–129. (2015) 638 DOI:10.1016/j.anucene.2014.08.048

639 [7] Romano, P.K., Horelik, N.E., Herman, B.R. *et al*, OpenMC: 640 A state-of-the-art Monte Carlo code for research and de- 641 velopment. *Ann. Nucl. Energy* 82, 90–97. (2014) DOI: 642 10.1016/j.anucene.2014.07.048

643 [8] Deng, L., Ye, T., Li, G. *et al*, 3-D Monte Carlo Neutron–Photon 644 Transport Code JMCT and Its Algorithms. PHYSOR 2014, 645 Kyoto, Japan, September 28–October 3, 2014

646 [9] Horelik, N., Herman, B., Forget, B. *et al*, Benchmark for eval- 647 uation and validation of reactor simulations (BEAVRS). *Intl.* 648 *Conf. Mathematics and Computational Methods Applied to* 649 *Nuclear Science & Technology* (M&C 2013); 2013 May 5–9; 650 Sun Valley.

651 [10] Chen, G., Jiang, X., Wang, T. *et al*, Development of a GPU- 652 based numerical reactor physics code CRANE. 19th Reactor 653 Numerical Computation and Particle Transportat Conference, 654 Shanghai, 2023. (in Chinese)

655 [11] Zhang, S., Chen, G., Development of a new lattice physics code 656 robin for PWR application. *Intl. Conf. Mathematics and Com- 657 putational Methods Applied to Nuclear Science & Technology* 658 (M&C 2013); 2013 May 5–9; Sun Valley.

659 [12] Salko, R., Wysocki, A., Blyth, T. *et al*, CTF: A 660 modernized, production-level, thermal hydraulic solver for 661 the solution of industry-relevant challenge problems in 662 pressurized water reactors. *Nucl. Eng. Des.* 397. (2022) 663 DOI:10.1016/j.nucengdes.2022.111927

664 [13] Cong, T., Chen, H., Chen, C. *et al* Development and 665 evaluation of fuel performance analysis code FuSPAC. *Int.* 666 *J. Adv. Nucl. React. Des. Technol.* 4, 129–138. (2022) 667 DOI:10.1016/j.jandt.2022.08.002

668 [14] Yamamoto, A., Tabuchi, M., Sugimura, N. *et al*, Deriva- 669 tion of Optimum Polar Angle Quadrature Set for the Method 670 of Characteristics Based on Approximation Error for the 671 Bickley Function. *J. Nucl. Sci. Technol.* 44, 129–136. (2007) 672 DOI:10.1080/18811248.2007.9711266

673 [15] Rombough, C.T., Adam, P.D., Attard A.C. *et al*, American Na- 674 tional Standard Reload Startup Physics Tests for Pressurized 675 Water Reactors. American Nuclear Society - ANS; La Grange 676 Park (United States); ANSI/ANS-19.6.1-2011.

677 [16] Kumar, S., Liang, J., Rathbun, M. *et al*, Inte- 678 gral Full Core Multi-Physics PWR Benchmark 679 with Measured Data NEUP 14-6742: Final Report. 680 <https://www.osti.gov/servlets/purl/1432668>

681 [17] Collins, B., Godfrey, A., Stimpson, S. *et al*, Simulation of the 682 BEAVRS benchmark using VERA. *Ann. Nucl. Energy* 145, 683 107602. (2020) DOI:10.1016/j.anucene.2020.107602

684 [18] Wang, K., Liu, S., Li, Z. *et al*, Analysis of BEAVRS 685 two-cycle benchmark using RMC based on full core de- 686 tailed model. *Prog. Nucl. Energy* 98, 301–312. (2017) 687 <https://doi.org/10.1016/j.pnucene.2017.04.009> DOI:10.1016/j.pnucene.2017.04.009

688 [19] Ryu, M., Jung, Y.S., Cho, H.H. *et al*, Solution of the 689 BEAVRS benchmark using the nTRACER direct whole core 690 calculation code. *J. Nucl. Sci. Technol.* 52, 961–969. (2015) 691 DOI:10.1080/00223131.2015.1038664

692 [20] Yu, J., Lee, H., Kim, H. *et al*, Simulations of BEAVRS 693 benchmark cycle 2 depletion with MCS/CTF cou- 694 pling system. *Nucl. Eng. Technol.* 52, 661–673. (2020) 695 DOI:10.1016/j.net.2019.09.007

696 [21] Choi, N., Kang, J., Lee, H.G. *et al*, Practical acceler- 697 ation of direct whole-core calculation employing graphics 698 processing units. *Prog. Nucl. Energy* 133, 103631. (2021)

699 DOI:10.1016/j.pnucene.2021.103631 702  
700 [22] Lee, H.G., Kim, K.M., Joo, H.G., Development of 703  
701 scalable GPU-based direct whole-core depletion calcula-  
tion methods. Prog. Nucl. Energy 165, 104928.(2023)  
DOI:10.1016/j.pnucene.2023.104928